Acta Polytechnica CTU Proceedings **48**:15–21, 2024
https://doi.org/10.14311/APP.2024.48.0015

Published by the Czech Technical University in Prague

AGEING EFFECTS ON THE MECHANICAL PROPERTIES STABILITY OF 3D PRINTED MATERIAL UNDER COMPRESSION

Veronika Drechslerová*, Nela Krčmářová, Jan Falta, Tomáš Fíla

Czech Technical University in Prague, Faculty of Transportation Sciences, Konviktská 20, 110 00 Prague, Czech Republic

* corresponding author: drechver@fd.cvut.cz

Abstract. The paper deals with the examination of the ageing effects on the mechanical properties stability of 3D printed material via stereolithography under compression when subjected to various conditions, including UV radiation, X-rays, and the effects of time, from the opening of the bottle with the material to the 3D-printing process. The sets of samples under investigation were subjected to quasi-static and dynamic compression loading using an Split Hopkinson Pressure Bar. The aim of this paper is to investigate the long-term stability of the samples in terms of their mechanical properties and material behaviour and their degradation pattern. Despite the manufacturer's information, it was found that the mechanical behaviour of the printed samples was significantly affected by the ageing process.

Keywords: Stereolithography, ageing, mechanical properties, compression.

1. Introduction

The continuous development of additive manufacturing techniques, in particular 3D printing from polymers, for example, using the stereolithography (SLA) method, has led to an increase in the popularity and widespread use of these materials. The extensive range of newly available materials has facilitated the design of structural components with specific properties for use in a multitude of industries, including the production of engineering parts, biomedical implants, decorative items, orthodontic appliances, aerospace components, and automotive components, among others [1]. The popularity of SLA technology can be attributed to its advantages over other additive technologies. These include faster printing speeds, better resolution, affordable acquisition costs, and a relatively smaller environmental footprint [2]. Concurrently, the expansion of applications has led to an increased need to comprehend the behaviour of materials when subjected to diverse external conditions (ageing processes) and under varying loading conditions. The long-term stability and degradation of materials have become a fundamental issue, which is a crucial parameter for the safety of printed parts in practice.

The ageing of epoxy resins in the restoration of cultural monuments was investigated in a study [3], where the authors sought to mitigate the effects of photoageing of the resin through the addition of UV stabilisers. The authors of paper [4] examined the impact of UV lamp intensity during printing (known as grayscale printing) on the mechanical properties of bio-based epoxy resins, as well as the influence of varying the colour and wavelength of the UV lamp. Another study [5] addressed the stability and long-term durability of epoxy-based composites. The authors tested the use of micro- or nano-sized fillers to strengthen the composites.

The aim of this study is to investigate the effect of ageing processes on the mechanical properties of the printed material. In light of the potential for dynamic loading applications, it is imperative that the materials employed undergo testing under dynamic conditions. This study, therefore, focuses on the impact of ageing processes on the mechanical properties of the printed material under compression loading. The dynamic testing of the mechanical properties of the materials in question remains an under-explored area of research. The observed change in the behaviour of the materials under dynamic loading highlights the necessity for this type of testing. Additionally, the study examined the potential influence of the interval between the opening of the resin bottle and the printing process.

2. Materials and methods

2.1. Materials

The SLA method and a compatible commercially available resin (Aqua Blue, Phrozen, Taiwan) were selected for the production of the test samples. The samples were produced on a Sonic Mighty 4K resin printer (Phrozen, Taiwan) with a bottom-up architecture and an illumination source in the form of a monochrome LCD display (405 nm ParaLED Matrix 2.0), which ensures high-resolution printing at 52 μm. The printing layer height was set to 0.05 mm, with the exposure time for the bottom layer set at 30 seconds and the other layers set at 2.5 seconds [6]. The selected process and resin were chosen due to their potential for utilising previously measured data from quasi-static tests.

2.2. Sample preparation

For compression tests, an axisymmetric specimen was designed in accordance with ASTM D695-15 [7], with the dimensions of the bulk specimen adapted to align with the technical specifications of the loading apparatus. The bulk specimen with the appropriate dimensions is illustrated in Figure 1. In order to achieve the desired level of quality and a smooth printing process, the designed specimens were rotated by the 40° about the x and y axes and placed on supports before printing in the slicing programme [8]. The prepared samples were then printed using the aforementioned resin printer.

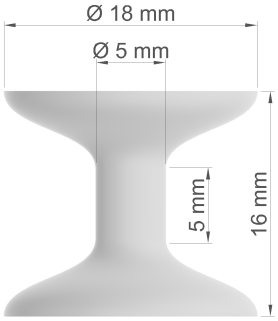

Figure 1. Basic dimensions of bulk specimen.

Subsequent to the printing process, the samples underwent post-processing, which involved cleaning in an ultrasonic bath and UV lamp curing for a period of 40 minutes. Figures 2 and 3 depict the printed sample and its surface detail, as observed via Scanning Electron Microscopy (SEM) with elemental volume representation according to spectral analysis: carbon ($66 \pm 2\,\%$) and oxygen ($33 \pm 2\,\%$). For the SEM observations, an accelerating voltage of 10 kV was employed, with a working distance of 10 mm. Given that the observed samples were composed of polymer, they were investigated in low vacuum mode with 200× resolution. Figure 3 illustrates a detail of each printed layer, with colour highlighting of printing imperfections, including irregularities in the surface of each layer and cured resin particles in an inconvenient location.

Figure 2. Printed bulk specimen.

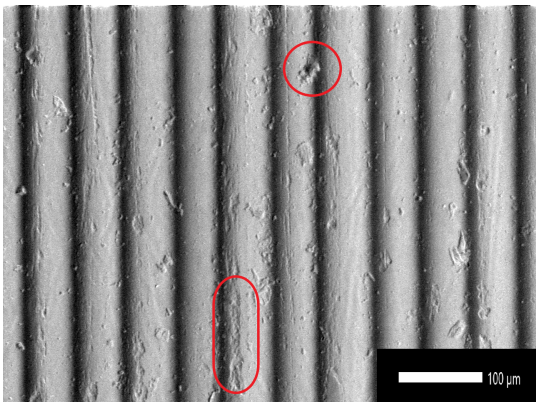

Figure 3. Detail of the sample surface by SEM.

2.3. Ageing process

A new resin was used to produce the samples to avoid interference due to the time delay between opening the bottle of material and production. The selection of the type of ageing was determined by the availability of laboratory equipment and the potential effects to which the printed parts may be subjected in real-world applications. In consideration of the aforementioned circumstances, the sets of samples were subjected to:

- sunlight,
- X-rays.

A total of 80 samples were subjected to sunlight, with sets of samples tested after one week and less than a month. In the present study, a total of 40 samples were tested, of which 20 were used for evaluation. These samples were divided into four sets of five according to the duration of exposure to sunlight and the type of test. The remaining samples were comprised of erroneous measurement samples and calibration samples.

A total of 24 samples were subjected to X-ray radiation for a duration of 2 and 4 hours. Subsequently, all the exposed samples were subjected to testing, and 20 representative samples were selected and divided into four sets of five samples each. The employed X-ray tube type was Comet MXR 225 HP 11 (Comet X-ray, Switzerland) was sealed chamber, tungsten target and dual focal spot size option. The X-ray irradiation procedure used acceleration voltage of 50 kV and emission current of 30 mA resulting in nominal output power of 1500 W. The tube has standard tungsten target energy spectrum with a near-conical beam with angle geometry of 30×40 degrees. The specimens were placed on a rotating platform with the rotation axis at a distance of 1 m from the focal spot. Shielding from X-radiation at this settings and distance was approximately $3.75 \cdot 10^7$ photons $\mathrm{mm}^{-2}\,\mathrm{s}^{-1}$. The dose rate was approximately ($9.25\,\mathrm{Sv\,h}^{-1}$), see BS 4094-2:1971 – Recommendation for data on shielding from ionizing radiation.

Additionally, the impact of the time elapsed between the opening of the resin bottle and the printing process was evaluated, with a time interval of six and

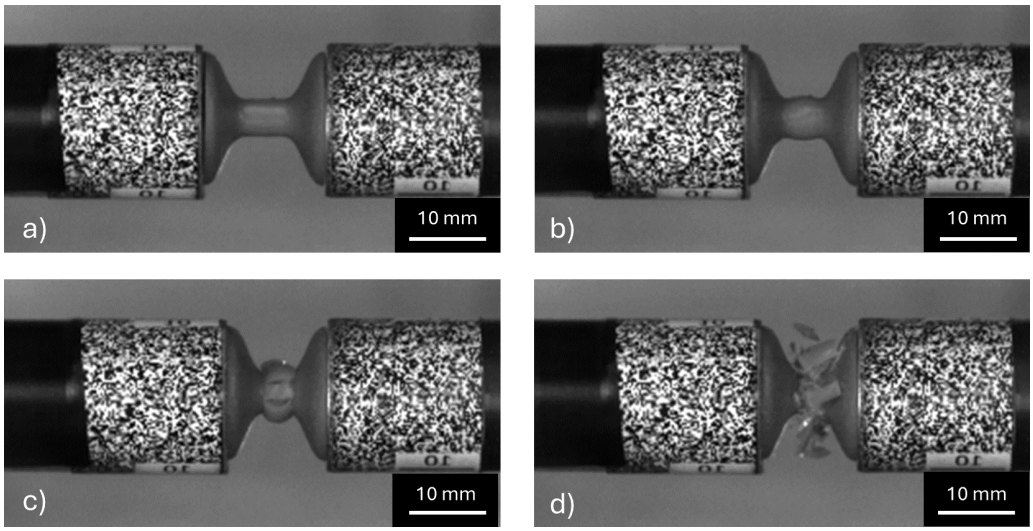

FIGURE 4. Photographs showing the progressive destruction of a specimen during a dynamic compression test.

ten months post-opening. In this instance, 12 samples were generated for each time period under examination, and once more, 20 samples were selected from the aforementioned samples, which were then divided into four sets of five samples in accordance with the elapsed time from resin opening to production and the type of test.

In order to facilitate a comparison with the measured data and to demonstrate the extent of the effects of ageing, two sets of five samples was produced that were not subjected to any ageing process and tested immediately after the manufacturing process (including post-processing).

2.4. Experimental procedure

In order to obtain the necessary data to determine the load behaviour and mechanical properties, a total of 14 sets of five specimens in each set (70 bulk specimens) were used. The requisite data for each sample was recorded prior to measurement for subsequent incorporation into the evaluation. Two testing methods were employed:

- quasi-static compression test,
- dynamic compression test (impact test).

The quasi-static test was conducted on an Instron 3382 universal loading machine, where the specimens were subjected to uniaxial compression. The quasi-static experiments were conducted using loading velocity of $1\,\mathrm{mm\,min^{-1}}$ resulting in the nominal strain rate of $300\,\mathrm{s^{-1}}$. The test was carried out until a steep force drop was observed, indicating specimen failure.

As the experimental campaingn required several months to be completely finished, the experimental setup for dynamic testing could not be kept identical due to other measurements performed in the laboratory. For this reason, two versions of the Split Hopkinson Pressure Bar (SHPB) were employed: the standard SHBP and a modified Direct Impact Hopkinson Bar (DIHB). In all the experimental setups, the parameters of the experiment were set identical with the average strain rate approximately $1600–1800\,\mathrm{s^{-1}}$, an incident bar of 20 mm diameter and 1600 mm length and a transmission bar of the same diameter and 2100 mm length were used. The striker bars employed were 750 mm in length at 2.0 bar gas-gun pressure and 648 mm in length at 1.8 bar gas-gun pressure [9]. The impact velocities were approximately $15\,\mathrm{m\,s^{-1}}$. A high-speed camera was installed during the measurements to obtain an image record of the test sample. In all the experiments, a frame rate of the camera was set to 300 kfps. The acquired image recordings during the dynamic test are presented in Figure 4. Figure 4a illustrates the initial sample location at $0\,\mu$s. Figure 4b shows the sample at $262\,\mu$s from impaction, with a displacement of 1.75 mm. Figure 4c illustrates the violation of the observed sample region at $349\,\mu$s, with a displacement of 2.88 mm. Figure 4d demonstrates the complete deformation of the observed central region of the sample at $396\,\mu$s from impaction, with a displacement of 3.25 mm.

2.5. Data evaluation

The evaluation of the measured data was conducted in MATLAB (MathWorks, Inc., USA) in order to obtain the mechanical properties of the material and to generate and compare stress-strain plots. The data obtained from the quasi-static test did not require any pre-processing and could be utilised immediately.

Dynamic experiments using the SHPB apparatus were evaluated using data of the strain-gauges and standard one-dimensional wave propagation theory. The DIHB experiments were evaluated similarly to the method described in [10] while only displacement and velocity data were available at the input side. Data from all the sensors were time-shifted to the bar's boundary with the specimen where corresponding force, displacement and velocity quantities were

evaluated. When data from redundant sensors were available they were averaged. Wave dispersion effects in the SHPB experiment were extensively reduced by a thin soft copper pulse shaper placed at the impact side of the incident bar. Overall, very good dynamic equilibrium conditions with almost constant strain rate were achieved in the experiments during as is demonstrated in Figure 5.

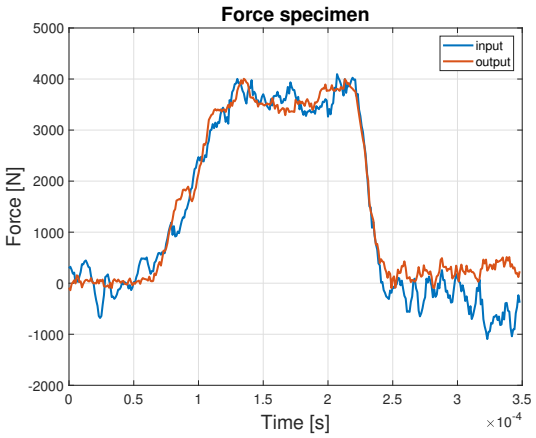

Figure 5. Typical dynamic equilibrium of the SHPB.

As the disintegration of the specimen occured always during the first impact wave in the experiment, the results of the SHPB and DIHB experiments are comparable. Typical strain rate during the experiment plotted against specimen's displacement is shown in Figure 6 and typical dynamic equilibrium of the SHPB experiment is presented in Figure 5. Experiments carried out using the DIHB were of single-sided strain-gauge instrumentation on the output side. The input side was instrumented by the displacement/velocity sensor only. Therefore, it was not possible to evaluate force at the input side of some experiments and the equivalent graph for the DIHB experiment is not presented here.

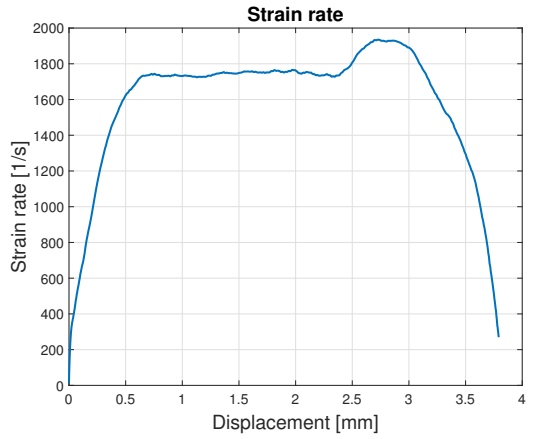

Figure 6. Typical strain rate during the experiment.

A number of evaluation scripts were employed to calculate the generation of the diagrams and compute basic mechanical properties, including Young's modulus in compression E, compression strength σ_{U}, yield stress σ_{Y} and relative shortening ϵ_{tb}.

The resulting curves displayed in the stress-strain diagrams represent the mean curves corresponding to each set of specimens. In the comparison diagrams, the curve corresponding to the specimens tested immediately after manufacture is taken as the reference curve and compared with the other average curves of the individual sets of specimens subjected to ageing processes. Furthermore, the plots display the standard deviation in transparent coloured areas around each curve, which indicates the variability of the measured data for each test sample in the set.

3. Results

3.1. Quasi-static compressive loading

A comparison of the stress-strain diagrams reveals significant differences between the curves representing samples exposed to sunlight (Figure 7a) and open resin (Figure 7b) and those not exposed to any ageing effect. The values of yield stress and ultimate strength are notably higher in the former. The average yield stress increased by approximately 76 % for the sets exposed to sunlight and by 37 % for the open resin. The ultimate compression strength decreased by approximately 12 % for the open resin samples in the comparison, while it remained almost identical for the other set (with a difference of 1 %).

In the case of X-ray exposure of the samples (Figure 7c), the data demonstrate that differences in the engineering stress-strain curves emerge at strain values above 60 %, while at lower strain values the curves are similar. This finding is consistent with the differences in the average compressive strength values, which indicate a reduction in yield stress and ultimate strength of approximately 18 % and 15 %, respectively.

3.2. Dynamic compressive loading

Upon examination of the individual engineering stress-strain diagrams, it becomes evident that the diagrams exhibit greater variability than was observed in the quasi-static tests. In comparison to the average curve of the set of tested specimens immediately after fabrication, the specimens exposed to sunlight for a period of seven days exhibited higher values for both yield stress (by approximately 12 %) and ultimate strength (by 28 %). The specimens that were exposed for 25 days exhibited higher values for yield stress and ultimate strength, with increases of approximately 45 % and 20 %, respectively (Figure 8a). The average curves corresponding to the specimens made of open resins (Figure 8b) exhibited an increase in the average values of yield stress and ultimate strength of approximately 16 % and 18 %, respectively. Additionally, a significant difference in the maximum strain achieved was observed, reaching approximately 40 % for the aforementioned sets.

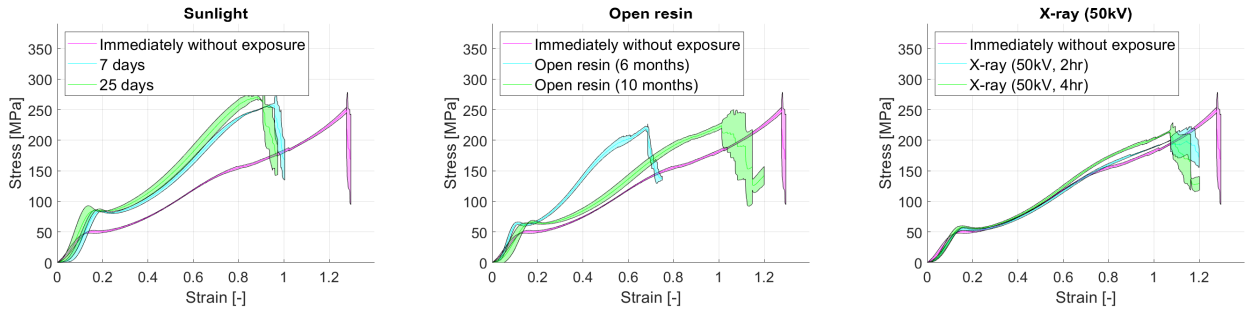

(A). (B). (C).

FIGURE 7. A comparison of the resulting engineering stress-strain curves for quasi-static compression loading.

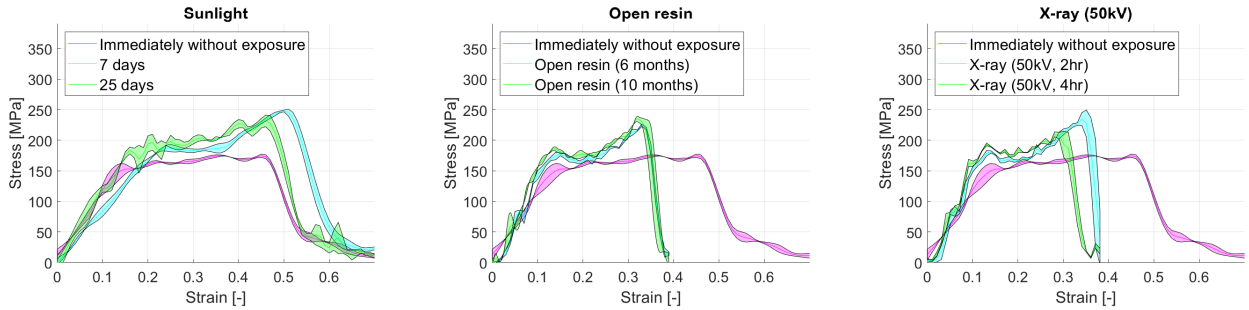

(A). (B). (C).

FIGURE 8. A comparison of the resulting engineering stress-strain curves for dynamic impact loading.

In the case of samples that have been exposed to X-rays (Figure 8c), a similar behaviour of the samples during the test can be observed as for samples made of open resin, although with a greater difference in the curves depending on the time of exposure to radiation. The yield stress and strength values of the samples tested after an exposure time of two hours were found to be approximately 12 % and 23 % higher, respectively. For the samples tested after an exposure time of four hours, the yield stress and strength values are approximately 21 % and 8 % higher, respectively.

3.3. Comparison of quasi-static and dynamic loading

The basic mechanical properties were calculated from the measured data, both for quasi-static loading and for dynamic loading, and entered into the Table 1 and Table 2. Concurrently, comparative plots of quasi-statics versus dynamics were constructed for each type of aging. The selected plots are presented in Figure 9. The achieved values demonstrate that the average yield stress values for quasi-static testing are significantly lower than those for dynamic testing, with a difference of up to 77 % in the framework. With regard to the strengths, it can be stated that in the majority of cases, the relative difference is up to 5 % on average. Furthermore, it is evident from Table 2 that the calculated mechanical parameters exhibit relatively high standard deviations, which can be attributed to the inherent variability of the individual measured data.

4. Conclusions

As part of the study, sets of printed samples were subjected to three different ageing effects using stereolithography: sunlight, X-rays, and the effect of the time elapsed between the opening of the resin and its use for production. The long-term stability, degradation, and changes in mechanical properties of the samples were investigated in accordance with the type of ageing. In order to plot stress-strain diagrams and determine the values of the basic mechanical properties, the samples were subjected to destructive loading tests in the form of compression quasi-static and dynamic tests.

The results of the study indicated that the long-term stability of the material was affected by the action of ageing processes. The sets of samples exhibited disparate mechanical behaviours under loading, resulting in markedly disparate values for the mechanical properties. For sunlight, it was observed that large changes in mechanical properties occur during the first week of ageing, after which the changes become negligible with increasing exposure time. The study of the effect of opening the resin bottle showed different behaviour for quasi-static and dynamic loading. While for the dynamic compression test, a similar trend could be observed over the course of the test for specimens made from already-opened resin, for the quasi-static test, the data varied depending on the time the resin bottle was opened. For the samples exposed to X-rays, no significant difference was observed as a function of the time the samples were exposed.

Aging	Mechanical characteristic			
	E [MPa]	σ_Y [MPa]	σ_U [MPa]	ϵ_{tb} [%]
Immediately	1608.50± 20.02	45.60± 1.98	258.63± 11.17	1.55± 0.82
Sunlight (7 days)	2678.19± 20.43	80.35± 1.56	257.25± 1.96	6.47± 0.25
Sunlight (25 days)	3027.57± 88.02	83.07± 0.58	270.99± 3.46	5.07± 0.48
Open resin (6 months)	2095.65 ± 57.62	60.05± 2.79	220.89± 1.92	7.09± 0.37
Open resin (10 months)	2257.48± 67.88	63.62± 1.00	235.23± 6.94	6.81± 0.42
X-ray (50 kV,2 hr)	1816.69± 33.38	50.70± 2.77	209.20± 7.08	6.79± 0.64
X-ray (50 kV,4 hr)	1983.25± 32.36	54.87± 1.62	220.28± 6.89	6.80± 0.51

Table 1. Quasi-static compression test – mechanical characteristic values.

Aging	Mechanical characteristic		
	E [MPa]	σ_Y [MPa]	σ_U [MPa]
Immediately	1846.77± 18.29	159.53± 23.77	194.91± 16.81
Sunlight (7 days)	1118.87± 71.45	173.49± 11.59	248.53± 0.57
Sunlight (25 days)	1175.46± 15.07	218.60± 39.02	232.95± 3.75
Open resin (6 months)	1964.58± 140.48	174.48± 16.16	223.11± 1.32
Open resin (10 months)	1646.88± 180.23	183.79± 4.99	235.05± 1.34
X-ray (50 kV,2 hr)	1834.27± 69.71	175.63± 5.24	239.26± 12.48
X-ray (50 kV,4 hr)	2384.55± 133.07	187.11± 1.96	209.82± 6.79

Table 2. Dynamic impact test – mechanical characteristic values.

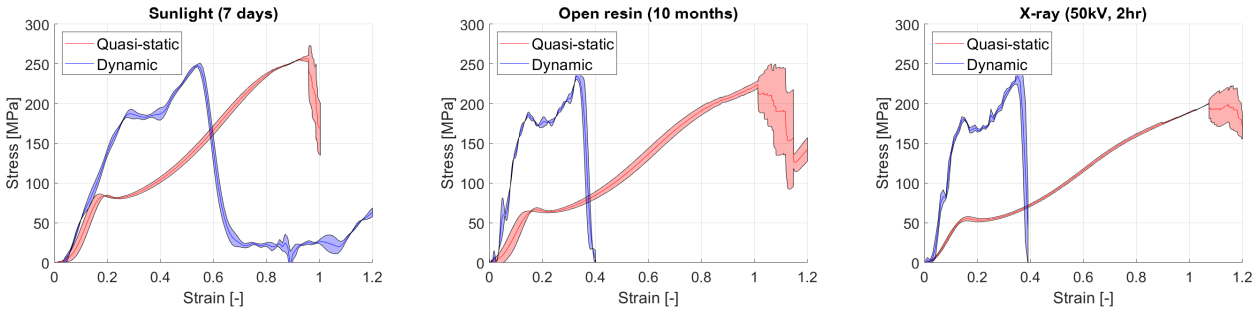

(a). (b). (c).

Figure 9. A comparison of the resulting engineering stress-strain curves for quasi-static and dynamic loading.

Acknowledgements

There is very appreciated a kind sponsorship of grants from Czech Science Foundation – Junior Star (project no. 22-18033M).

References

[1] M. I. Farid, W. Wu, X. Liu, P. Wang. Additive manufacturing landscape and materials perspective in 4D printing. *The International Journal of Advanced Manufacturing Technology* **115**(9–10):2973–2988, 2021. https://doi.org/10.1007/s00170-021-07233-w

[2] P. Sharma, H. S. Mali, A. Dixit. Mechanical behavior and fracture toughness characterization of high strength fiber reinforced polymer textile composites. *Iranian Polymer Journal* **30**(2):193–233, 2020. https://doi.org/10.1007/s13726-020-00884-8

[3] S. Jeong, N. C. Cho. A study on aging characteristics of epoxy resins for conservation treatment of cultural heritage by adding UV stabilizer. *Analytical Science and Technology* **24**(5):336–344, 2011. https://doi.org/10.5806/AST.2011.24.5.336

[4] M. Bergoglio, E. Rossegger, S. Schlögl, et al. Multi-material 3D printing of biobased epoxy resins. *Polymers* **16**(11):1510, 2024. https://doi.org/10.3390/polym16111510

[5] Z. Wang, X. Zhang, C. Cheng, et al. 3D printing of architectured epoxy-based composite lattices with exceptional strength and toughness. *Composites Part B: Engineering* **256**:110653, 2023. https://doi.org/10.1016/j.compositesb.2023.110653

[6] V. Drechslerová, M. Neuhäuserová, J. Falta, et al. Stereolithography for manufacturing of advanced porous solids. *Acta Polytechnica CTU Proceedings* **41**:1–7, 2023. https://doi.org/10.14311/app.2023.41.0001

[7] ASTM D695-15. Standard Test Method for Compressive Properties of Rigid Plastics. https://doi.org/10.1520/d0695-15

[8] V. Drechslerová, J. Falta, T. Fíla, et al. Effect of aging on mechanical properties of 3D printed samples using stereolitography. *Acta Polytechnica CTU Proceedings* **42**:1–5, 2023. https://doi.org/10.14311/app.2023.42.0001

[9] M. Neuhäuserová, P. Koudelka, T. Fíla, et al. Strain rate-dependent compressive properties of bulk cylindrical 3D-printed samples from 316L stainless steel. *Materials* **15**(3):941, 2022. https://doi.org/10.3390/ma15030941

[10] T. Fíla, P. Koudelka, J. Falta, et al. Dynamic impact testing of cellular solids and lattice structures: Application of two-sided direct impact hopkinson bar. *International Journal of Impact Engineering* **148**:103767, 2021. https://doi.org/10.1016/j.ijimpeng.2020.103767